Specific heat of amorphous rare-earth–transition-metal films

F. Hellman, E. N. Abarra,* and A. L. Shapiro
Department of Physics, University of California, San Diego, La Jolla, California 92093

R. B. van Dover
Lucent Technology, 600 Mountain Avenue, Murray Hill, New Jersey 07974
(Received 9 September 1997)

Microcalorimeters have been used to measure the temperature dependence of the specific heat $C_p(T)$ of amorphous R_xFe_{100-x} (R=Gd, Tb) thin films prepared by both sputtering and *e*-beam coevaporation. a-Tb_xFe_{100-x} films possess large randomly oriented local magnetic anisotropy and large exchange coupling; they are considered random-anisotropy magnets. By varying growth temperature and by annealing, films of the same composition but with very different *macroscopic* anisotropy constant K_u were prepared and studied. K_u reflects the degree of nonrandomness in the local anisotropy axis directions. a-Gd_xFe_{100-x} films possess negligible local and macroscopic anisotropy. All samples show a relatively sharp peak in $C_p(T)$ at the Curie temperature T_c determined by magnetization measurements, indicative of a phase transition, independent of the magnitude of K_u. Effective critical exponents of $\alpha=\alpha'=-0.6$ to -0.7 and a critical amplitude ratio of 1.5–2.5 are measured for reduced temperatures down to 0.02. Nearly all possible magnetic entropy is developed below T_c, unlike what is seen in spin glasses. Increased growth *or* annealing temperature causes a small but systematic increase in T_c, in the inverse high-field susceptibility χ and in the homogeneity of the sample; K_u by contrast increases with growth temperature, but decreases with annealing. [S0163-1829(98)09733-1]

I. INTRODUCTION

The structural and magnetic properties of amorphous rare-earth–transition-metal (a-R-TM) alloys and amorphous $TbFe_2$ in particular have been extensively studied over the last 20 years. The combination of a transition metal such as Fe or Co, which gives a high T_c (well above room temperature in many cases), and a rare earth such as Tb, which gives a large local magnetic anisotropy, causes the material to be of technological importance. For most thin films, the growth-deposition process induces a perpendicular uniaxial anisotropy K_u.[1–5] K_u together with a suitable T_c, coercivity, Kerr rotation, and optical reflectivity, has made quaternary alloys related to a-$TbFe_2$, the material of choice for magneto-optic recording.[6,7] Because of the strength and (approximately) random orientation of the local magnetic anisotropy field of the Tb ion, which tends to pull the local magnetic moment away from a collinear arrangement, studies of amorphous $TbFe_2$ were prominent in the development of random-magnetic-anisotropy (RMA) theory, a branch of the field of random magnetism.[8–20]

Specific heat studies of magnetic materials are useful in several ways: characterization of the nature of the magnetic transition, determination of the magnetic entropy evolved and hence the number of magnetic states populated between $T=0$ and the transition and/or above the transition, and characterization of the low-energy magnetic excitations of the system. Specific heat measurements allow a characterization of the magnetic transition and low-temperature properties in zero magnetic field, a useful property when magnetic measurements may be complicated by magnetic history dependence such as in spin glasses. It is also helpful to know the temperature dependence of the specific heat of a material used for magneto-optic recording where heating it from room temperature to above the magnetic ordering temperature is needed for what is called Curie point writing. There have been no specific heat studies of a-Tb-Fe alloys, largely due to the technical difficulties inherent in measuring the specific heat of thin films at temperatures at and above room temperature. Studies on RMA materials to date have focused on those with low magnetic freezing temperatures.[21–25] We have made recent advances in microcalorimetry which make high-temperature measurements possible.[26] In this paper, we present measurements of the specific heat $C_p(T)$ and high-field magnetic susceptibility $\chi(T)$ for a-RFe_2 (R=Tb, Gd) prepared under different conditions in order to clarify the effects of preparation conditions and the interplay of random anisotropy, exchange, and coherent uniaxial anisotropy on the magnetic state of these alloys.

The exchange interaction between Fe ions is primarily ferromagnetic (due to a relatively large Fe-Fe separation), while the interaction between R and Fe ions is antiferromagnetic [but not frustrated, since the two subnetworks of Tb (or Gd) and Fe are distinct], giving rise to a ferrimagnet (more properly termed a sperimagnet for a-$TbFe_2$ due to the random anisotropy of Tb). Comparisons to a-Y-Fe (Refs. 9 and 27) suggest that there is still significant exchange frustration from some antiferromagnetic Fe-Fe interactions, but these are somewhat offset by the R-Fe interactions which are not frustrated, making this a reasonably good system for studying random anisotropy effects. Harris, Plischke, and Zuckermann (HPZ) introduced the following Hamiltonian for RMA materials with predominantly ferromagnetic exchange: $H=-\frac{1}{2}J_{ex}\Sigma_{ij}\vec{S}_i\cdot\vec{S}_j-\frac{1}{2}D\Sigma_i(\hat{n}_i\cdot\vec{S}_i)^2-\vec{H}\cdot\Sigma_i\vec{S}_i$.[12] The first term is a Heisenberg exchange with average strength J_{ex}, the second is the random anisotropy term, and the third is the interaction with an external field $\vec{H}$. The anisotropy term

approximates the low symmetry of the amorphous structure with a uniaxial anisotropy of (average) strength D and direction $\hat{n}_i$, which varies from site to site. There have been a number of reviews of this problem, both theoretical and experimental.[11,13–15] It is generally believed that amorphous magnets with isotropically distributed RMA show no magnetic long-range order (LRO) for dimension $d \leqslant 4$ for three spin components ($m=3$), even for $J_{ex}>0$. This result has been rigorously proved in the large-D or large-m limit; arguments have been made that it also holds for infinitesimal D, but the low-D/J_{ex} limit is much less clear.[16–18,28]

Because of the strength of the Tb-Fe exchange and the strength of the local anisotropy constant D for Tb, $D/J_{ex} \sim 0.3-0.7$ for a-$TbFe_2$.[29] Small-angle neutron-scattering studies[8] on a-$Tb_{32}Fe_{68}$ (extremely rapidly sputtered, with no macroscopic anisotropy K_u) showed a noncollinear magnetic structure and a finite ferromagnetic correlation length below the transition temperature T_c; this result was pivotal in the early development of RMA theory. The correlation length increased from ~10 Å at 450 K to only ~135 Å below $T_c = 409$ K, and then decreased to ~50 Å at low temperature. Further evidence of the random-anisotropy state in a-$TbFe_2$ was a large high-field susceptibility χ above technical saturation and a reduced value of the Tb saturation moment.[8,9]

For $D/J_{ex} \gg 1$, theory and simulation show an exponentially damped spin-spin spatial correlation function, with a finite ferromagnetic correlation length R_f, which is short, but considerably larger than the lattice constant a, and zero net magnetization in zero field.[18,28,30] This state has been termed speromagnetic and has zero macroscopic moment. The transition from the high-temperature paramagnetic to the low-temperature spin-frozen state has been shown theoretically to be related to that of an exchange-frustrated spin glass, where at most high-order derivatives of the free energy show discontinuities. Monte Carlo simulations by Jayaprakash and Kirkpatrick showed a broad parabolic peak in $C_p(T)$ at a temperature far above any magnetic freezing, consistent with the development of short-range magnetic order as is commonly seen in exchange-frustrated spin glasses.[18]

The weak anisotropy limit $D/J_{ex}<1$ is theoretically less clear. Between the $D=0$ ferromagnetic state and the $D/J_{ex} \gg 1$ nonferromagnetic state, there must be a phase transition at some value of D/J_{ex}. This could occur at exactly $D=0$, the spin correlations remaining exponentially damped with a correlation length R_f which increases as D/J_{ex} becomes smaller and becomes infinite as D approaches zero (to be more precise, limited only by long-range dipolar effects as in a conventional ferromagnet). There has been a suggestion that for small D/J_{ex}, the behavior at T_c might resemble that of a simple ferromagnetic system, with the RMA properties not being relevant until magnetic order is well developed.[15,20] Alternatively, there could be a crossover at a finite D/J_{ex} value. A likely scenario, based on results of Fisch described below,[31] is that there are two crossovers: one at $D=0$ from true long-range ferromagnetic order to a quasi-long-range-ordered state with power-law spin correlations for finite but small D/J_{ex} and a second crossover at larger D/J_{ex} to the exponentially damped spin correlation state described above. It is experimentally clear that the ratio of D/J_{ex} has a strong impact on magnetic properties such as coercivity and high-field susceptibility, with a crossover between different types of behavior (exchange dominated versus anisotropy dominated) suggested to be at $D/J_{ex}=0.3$.[11,32,33] If there is a critical value of D/J_{ex}, it would necessarily depend on the concentration of the rare earth in the alloy, as well as on the crystal structure which affects the number of neighbors.

As an approximation to a low-D/J_{ex} material, Fisch recently performed a computer simulation for a two-component RMA material, one with $D/J_{ex}=\infty$ and concentration x and the other component with $D/J_{ex}=0$. This simulation shows a crossover from spin-glass behavior at high x to a quasi-long-range-ordered (QLRO) state for $x<0.6$, suggesting that low-D/J_{ex} materials might exhibit this QLRO state.[31] Fisch also found a QLRO state for spins confined to a plane ($m=2$), in three dimensions ($d=3$) even for $D/J_{ex} \gg 1$,[34] and in the related random-field problem in $d=3$.[35] The QLRO state has no true long-range magnetic order, but has power-law spin-spin correlations (instead of exponentially damped) and a susceptibility and correlation length which diverge at the phase transition from the paramagnetic state. The critical behavior of specific heat in this $d=3$, $m=3$ RMA model is still not completely clear; it appears that extremely small reduced temperatures ($t=|T-T_c|/T_c$) may be necessary to observe true critical behavior and that the applicable range of reduced temperature shrinks with reducing x. The manifestation of this behavior is that the apparent critical behavior depends on the value of x. For example, at $x=0.125$, Fisch found that the specific heat exhibited a cusp with critical exponent $\alpha \sim -0.45$ and amplitude ratio $A/A'=2.5$ to as small a reduced temperature as was compatible with the size of the simulation, while at $x=0.25$, a reasonable approximation to a-$TbFe_2$ since D/J_{ex} is of order 0.7 for Tb, the specific heat appeared to exhibit a cusp with $\alpha \sim -0.6$ and $A/A'>1$, down to reduced temperatures of 0.05, below which deviations occurred. For $x=0.5$ (more appropriate for a-Tb_2Fe), the peak is rounded ($\alpha<-1$). This variation with x is an indication that the observations actually reflect crossover behavior (from pure Heisenberg to the real RMA). The true critical behavior at the transition to the QLRO state for $m=3$, $d=3$ is (probably) a broad peak with α between -1 and -2, but will only be observable extremely close to T_c for most x. The $m=2$, $d=3$ RMA problem shows a cusp in the specific heat (hence a discontinuous derivative), like a Kosterlitz-Thouless phase, with critical exponents $\alpha=\alpha'=-0.76$ and $A/A'=1$.[34]

Experimental low-temperature specific heat studies on a-$DyCu_2$ and a-$Dy_{52}Cu_{48}$ show broad transitions characteristic of spin glasses.[21–23] In these materials, however, significant exchange frustration almost certainly exists and may play a crucial role. By contrast, specific heat data by von Molnar *et al.* and Hattori *et al.* on a-$Dy_{32}Ni_{68}$ and a-$Er_{33}Ni_{67}$ alloys (both with T_c below 20 K and large but not infinite D/J_{ex} and no significant exchange frustration) show a relatively narrow maximum at a temperature T_c similar to that measured magnetically.[25,24] We have fit their data to critical exponents and find reasonable scaling with $-2<\alpha=\alpha'<-1$, consistent with the theoretical work by Fisch.

Magnetic measurements near and at the magnetic freezing temperature by Sellmyer and Nafis, Dieny and Barbara, Lee

and O'Shea, and others showed that the ac magnetic susceptibility grows large over a narrow temperature range and the nonlinear susceptibility appears to diverge at the freezing temperature for $m=3$, $d=3$ materials even for large (but not infinite) D/J_{ex}, also consistent with Fisch's recent work.[9,11,14,32,36–42] These data have been interpreted as showing a true phase transition, with critical exponents somewhat different than those found for the classical spin-glass materials,[39,40] consistent with the observations of specific heat.[24,25] There is also evidence of a crossover from spin-glass-like to ferromagnetic behavior as a function of increasing applied magnetic field.[36,41,42] There are, however, still questions concerning the interpretation of the critical exponents obtained from the fits to magnetization measurements. They depend nearly linearly on D/J_{ex},[36] which is not consistent with a critical point, since, in general, there cannot be continuously varying classes of exponents for similar materials. Reported critical exponents obtained by magnetization measurements together with scaling relationships give values of the specific heat critical exponent α ranging from -5 to >0.[36,39,40,43] These results are suggestive of Fisch's interpretation of crossover behavior giving different apparent values of critical exponents.[31]

An additional consideration in RMA materials is that the set of local anisotropy axis directions $\hat{n}_i$ is not necessarily random from site to site. There are two distinct types of correlations in $\hat{n}_i$, with different effects on the magnetic properties. First, there can be correlations in the directions of neighboring $\hat{n}_i$, introducing what Chudnovsky referred to as an orientational correlation length R_a.[20] It has been suggested that in the amorphous state, the orientational correlation length could and/or should be much longer than the positional correlation length, which tends to be only an interatomic distance a.[44] Following Chudnovsky's notation, R_a causes the exchange energy J_{ex} to be replaced by an effective exchange energy which is reduced by $(a/R_a)^2$. R_a therefore greatly impacts the crucial ratio of anisotropy to exchange energy, the ferromagnetic correlation length, and $M(H,T)$,[20,45,46] but in principle has no effect on the nature of the phase transition, *unless* the ratio of D/J_{ex} actually causes a change in universality class. R_a has never been determined by direct structural methods but magnetization studies of a-RFeB suggested an $R_a \sim 100$ Å, far greater than the ~ 10 Å atomic-structural correlation length.[45]

The second type of correlation in $\hat{n}_i$ is a preference for a given spatial direction, e.g., along the growth direction of a thin film, leading to a macroscopic anisotropy K_u. This type of correlation could have a much more profound effect; it has been theoretically demonstrated that even in the large-D/J_{ex} limit, the ferromagnetic state can be recovered as the ground state in the presence of sufficiently large but finite K_u.[19,20] It is clear that in the limit that *all* $\hat{n}_i$ are aligned along the growth direction, the material is a ferromagnet. There must therefore be a crossover at some fraction of $\hat{n}_i$ alignment. The nature of the magnetic freezing transition in the presence of large uniaxial anisotropy is not clear. If the ground state of the system is a ferromagnet with uniaxial anisotropy, it should have the critical parameters of the pure Ising system, for which the specific heat diverges ($\alpha>0$). The Harris criterion, however, says that $\alpha>0$ is not possible for a system with disorder, such as an amorphous material.[47] It is then not clear what critical exponents are expected; a possibility is those for the random-exchange Ising system, which has $\alpha=-0.1$ for $d=3$.

Experimental studies where D/J_{ex} was held at least approximately constant and the coherent anisotropy K_u changed in a controlled way are quite limited. del Moral *et al.* studied this transition in a disordered crystalline alloy ($Dy_xY_{1-x}Al_2$; the anisotropy D is due to random strain fields) as a function of increasing x, which increases D/J_{ex}.[48] Saito *et al.* examined the effect of coherent anisotropy on susceptibility in an a-$Dy_{10}Gd_4Fe_{86}$ alloy by choosing two films with different K_u; the source of the difference was not explained.[49] Qualitatively, it is known that the magnitude of K_u in a-$TbFe_2$ strongly affects the shape of the $M(H)$ hysteresis loops, but there have been no quantitative experimental studies of how the nature of the phase transition depends on K_u. Previous attempts to analyze the magnetic phase transition of a-$TbFe_2$ with perpendicular anisotropy K_u were unsuccessful; the material appeared to be multiphase.[43]

To consider the magnitude of K_u necessary to induce a crossover, we follow Chudnovsky's work and introduce the ratio $H_u/H_s = K_u A^3/K_r^4 R_a^6 = K_u R_f^2/A$ where $H_s = H_r^4/H_{ex}^3 = 2K_r^4/A^3 M_0 R_a^6$ is a characteristic crossover field for the material, $R_f = (A/K_r)^2\ 1/R_a^3$, and $H_u = 2K_u/M_0$ is the coherent anisotropy field.[20] When $H_u/H_s<1$, the properties of the RMA magnet are not significantly altered by K_u; for example, R_f is still given by the equation above. However, when $H_u/H_s>1$, the system is converted to what is called a ferromagnet with wandering axis. Here, the magnetization approximately lies along one of the two coherent anisotropy easy-axis directions, as in a conventional uniaxial ferromagnet, but within a domain, the magnetization wanders in direction with a characteristic tilt angle (away from the coherent anisotropy direction) $\sim (H_u/H_s)^{1/4} \propto (a/R_a)^{3/2}$ and a perpendicular correlation length $R_f^{\perp} \sim R_a (H_{ex}/H_u)^{1/2} = (A/K_u)^{1/2}$.

Previous work on a-$TbFe_2$ thin films has shown that the coherent anisotropy K_u increases with increasing substrate temperature T_s during deposition, from less than 1×10^6 erg/cm^3 to greater than 1×10^7 ergs/cm^3.[2,50] Annealing at temperatures near 620 K can reduce or eliminate this anisotropy, without inducing crystallization.[5,50,51] The magnitude of K_u can thus be varied over two orders of magnitude by choice of deposition conditions and/or annealing. Estimates of the necessary value of K_u needed to restore LRO are $\sim 4 \times 10^6$ ergs/cm^3 at low temperature and several times lower at room temperature.[52] The properties of an initially high K_u sample should therefore depend strongly on annealing, which reduces and then eliminates K_u (in which state the sample should be describable as an $m=3$, $d=3$ RMA material). With further annealing, tensile strains plus magnetostriction together with dipolar (shape) anisotropy make K_u significantly negative ($K_u<0$ means a planar anisotropy, which should be describable as an $m=2$, $d=3$ RMA state). These alloys should therefore be appropriate for examining the effect of coherent anisotropy on the RMA state and on the transition from paramagnetic to spin frozen state, similar to crystalline materials with magnetocrystalline anisotropy where the phase transition from paramagnet to ferromagnet

is strongly affected by the magnetocrystalline anisotropy.[53] Note that, both K_u and K_r must have the same temperature dependence since they have the same underlying source in the local electrostatic fields; therefore either neither or both are important to the nature of the phase transition.

II. SAMPLE PREPARATION AND CHARACTERIZATION

Samples were grown from separate Tb, Gd, and Fe sources by either *e*-beam coevaporation in a UHV chamber or by magnetron cosputtering with a Meissner (LN_2-cooled) shroud providing a high-vacuum environment. Nb or Cu were used as overlayers to prevent oxidation. The pressure before evaporation is $<3\times10^{-9}$ Torr and $<1\times10^{-8}$ Torr during growth; pressures during sputtering inside the Meissner shroud are similarly low. Samples were grown on substrates held at different temperatures T_s to obtain different values for the perpendicular anisotropy K_u. Typical deposition rates were 0.5–5 Å/s. There has been extensive x-ray scattering, transmission electron microscopy (TEM), neutron scattering, and extended x-ray absorption fine structure (EXAFS) studies on sputtered *R*-TM alloys in the past showing the amorphous nature of the samples and the absence of nanocrystallites.[1–3,5,8,54] X-ray, TEM, Rutherford backscattering, and Auger profiling studies have been performed on both our *e*-beam-evaporated and sputtered samples.[51,55] For *e*-beam-evaporated a-$Tb_{28}Fe_{72}$ grown at 523 K, the bright field TEM image is featureless and the selected area diffraction (SAD) rings are diffuse. TEM images for a-$Tb_{28}Fe_{72}$ grown at room temperature show diffuse SAD rings. For these samples, the bright field image shows evidence of density fluctuations with a length scale of 100–300 Å, presumably related to a columnar microstructure. Such microstructure is common in evaporated amorphous materials and is not evident in the sputtered films, nor in the evaporated films grown at 523 K.[56] Films grown at room temperature and annealed at 523 K appear identical in TEM to the as-deposited films, including the density fluctuations; in particular, no sign of crystallization was detected, consistent with earlier work on annealed a-Tb-Fe.[2,5] Auger depth profiling showed no O (to the resolution of the measurement, ~1%) in a-$Tb_{28}Fe_{72}$ and uniform Tb/Fe composition for both sputtered and evaporated samples.

Room-temperature magnetization and high-temperature *M* vs *T* measurements were made on a vibrating sample magnetometer. High-field susceptibility χ was measured in a superconducting quantum interference device (SQUID) magnetometer. K_u was determined using a torque magnetometer employing a 45° method.[57] Compositions were established by an electron microprobe,[58] with an uncertainty of ±1 at. %.

Heat capacity measurements of *microgram* thin films up to 540 K are made possible by the use of microcalorimeter,[26] which have an extremely small addenda (substrate, thermometer, and heater) contribution to the total heat capacity. The addenda is reduced by using a 180-nm-thick amorphous silicon nitride (a-Si-N) membrane as substrate, and using thin film heaters and thermometers. 2500 Å (17 μg) of Ag was first sputtered onto this membrane. This layer of Ag serves as a thermally conducting layer and makes the sample isothermal during measurement as discussed extensively in Ref. 26. The Ag layer is compressive because of the sputtering conditions; this prestressing of the device membrane was found to be necessary for the membrane to survive *e*-beam depositions of a-R_xFe_{1-x}, which are quite tensile for T_s <520 K.[59] For $T_s\sim520$ K, the tensile strain is smaller and we were able to use thermally evaporated (tensile) Au. The heat capacity of the Ag (Au) and device was first measured to give an accurate (<2%) determination of the addenda. The samples were then grown on the Ag (or Au) and, to prevent oxidation, capped with 30–50 nm of Cu (or Nb) evaporated *in situ*. As discussed in Ref. 26, we use the relaxation method in measuring the heat capacity. The measurements were carried out from 80 to 530 K in a high-temperature, high-vacuum cryostat. Sample masses were determined from the thicknesses, areas, and densities. Thicknesses were estimated from the deposition rates and compared with profilometry measurements made on films grown on a-Si-N-covered-Si substrates positioned next to the devices during sample deposition. Planar dimensions were measured using an optical microscope. We used previously reported values for the density of a-$Tb_{33}Fe_{67}$ of 8.3 g/cm^3 (Ref. 8) and a density of 8.3 g/cm^3 for a-$GdFe_2$. The film thickness (mass) for the heat capacity samples was typically 3000 Å (16 μg) to 4000 Å (21 μg) with an uncertainty of ±6%.

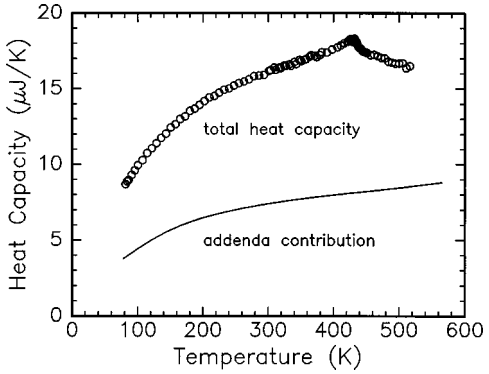

FIG. 1. Total heat capacity for microcalorimeter with a-$Tb_{32}Fe_{68}$ grown at 523 K (circles) and the contribution of addenda (Si-N substrate, thermometer, heater, and Au conducting layer) to this total (solid line).

III. RESULTS

Figure 1 shows the heat capacity of evaporated a-$Tb_{32}Fe_{68}$ grown at 523 K and the addenda (the nitride membrane substrate, thermometer, heater, and Au conducting layer). The total heat capacity at 500 K is ~17 μJ/K and the addenda contribution is ~8.5 μJ/K. Therefore, even at elevated temperatures when phonon contributions to the substrate heat capacity are most significant, the signal from ~21 μg of a-$Tb_{32}Fe_{68}$ is large. Subtracting the addenda contribution from the total signal gives the sample heat capacity (Fig. 2). For this high K_u (1.2×10^7 ergs/cm^3) sample, the transition is quite sharp (Fig. 2, lower inset). Annealing at 623 K for 4 h reduced K_u to $\sim3\times10^6$ ergs/cm^3. Measurement of the specific heat after annealing showed no significant change in the sharpness of the transition and a small increase in T_c (~5 K) (Fig. 2, upper inset).

Figure 3 shows the specific heat of evaporated a-$Tb_{32}Fe_{68}$

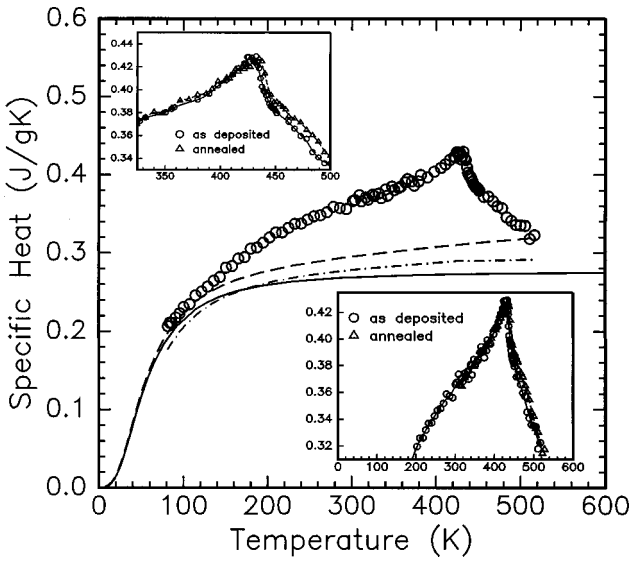

FIG. 2. Specific heat C_p for as-deposited e-beam-evaporated a-$Tb_{32}Fe_{68}$ grown at 523 K, after subtracting measured addenda and dividing by sample mass. Dash-dotted line: estimated lattice ($\Theta_D = 260$ K), electronic ($\gamma = 7$ mJ/mol K), and dilation (see Ref. 62) contributions. Solid line: Debye harmonic contribution for $\Theta_D = 230$ K. Long-dashed line: maximum lattice, electronic and dilation contributions, as discussed in the text. Top inset shows expanded x-axis scale of $C_p(T)$ as deposited (○) ($K_u = 1.2\times10^7$ ergs/cm^3) and annealed at 623 K (350 °C) for 4.5 h (Δ) ($K_u = 3\times10^6$ ergs/cm^3). Bottom inset shows same data with expanded y-axis scale.

grown at 348 K. $M = 300$ emu/cm^3 and $K_u \sim 1\times10^7$ ergs/cm^3. The transition appears less sharp and is shifted to slightly lower temperature than for the sample grown at 523 K (shown in Figs. 1 and 2). Annealing at 523 K for ~3 h made the macroscopic magnetic anisotropy in plane [$K_u < 0$ due to dipolar anisotropy (shape induced, $2\pi M^2$ for a thin film) and a tensile strain-induced magnetostrictive contribution]. $C_p(T)$ for this same sample after annealing shows a sharper peak and an increase in T_c of ~17 K (Fig. 3 and

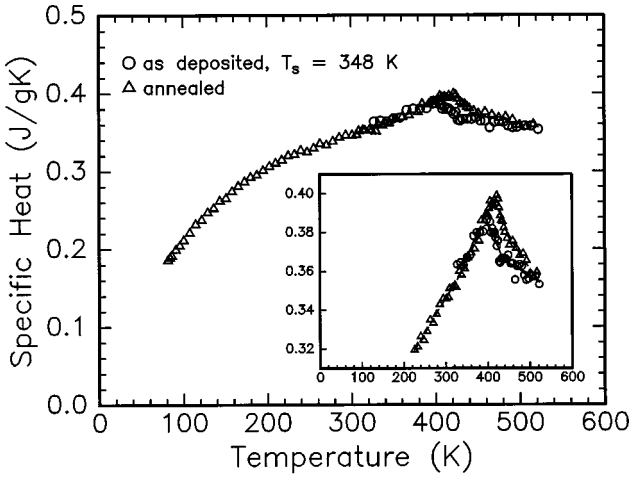

FIG. 3. Specific heat C_p for e-beam-evaporated a-$Tb_{32}Fe_{68}$ grown at $T_s = 348$ K as deposited (○) ($K_u \sim 1\times10^7$ ergs/cm^3, perpendicular to the film plane, $M = 300$ emu/cm^3) and (Δ) annealed at 523 K for 4.5 h (K_u in plane, M unchanged).

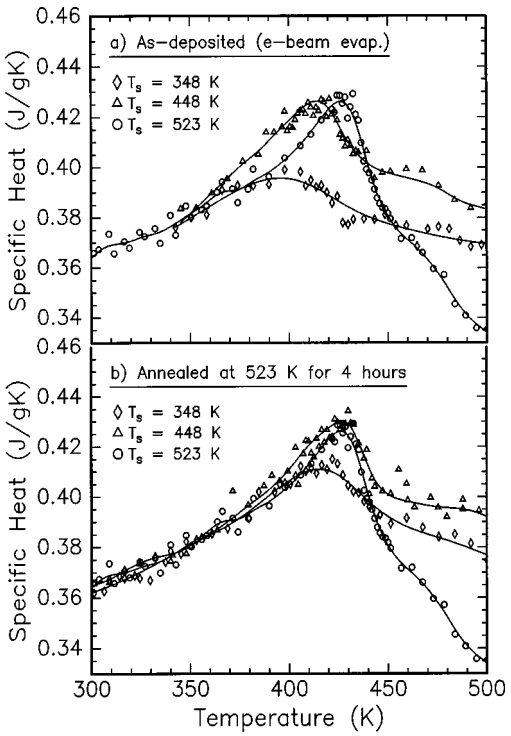

FIG. 4. Comparison of specific heat for e-beam-evaporated a-$Tb_{32}Fe_{68}$ grown at various temperatures: (a) as deposited, (b) annealed at 523 K for 4.5 h. Data are normalized to value of C_p at 350 K for sample grown at 523 K [C_p(measured)$\times$1.036 for $T_s = 348$ K as deposited, C_p(measured)$\times$1.021 for $T_s = 423$ K as deposited, C_p(measured)$\times$1.04 for $T_s = 348$ K annealed, C_p(measured)$\times$0.9895 for $T_s = 423$ K annealed].

inset expanded scale). Specific heat measurements for evaporated a-$Tb_{32}Fe_{68}$ grown at 423 K ($M = 350$ emu/cm^3, $K_u \sim 1.2\times10^7$ ergs/cm^3 as deposited and $K_u \sim 3\times10^6$ ergs/cm^3 annealed at 523 K for ~3 h) indicate very similar results (a sharpening of the transition and slight increase in T_c with annealing).[51]

Figure 4 shows a comparison of the specific heat of these e-beam-evaporated samples as deposited [Fig. 4(a)] and annealed [Fig. 4(b)]. Both annealing and higher deposition temperatures increase T_c and slightly sharpen the transition, despite the fact that they have opposite effects on K_u. The specific heat data become increasingly similar with annealing, suggesting that these samples relax toward the same homogeneous metastable amorphous state independent of preparation history.

Figure 5 shows the heat capacity of evaporated a-$GdFe_2$ grown at 348 K.[58] The specific heat shows a peak which is comparable in breadth to that of a-$Tb_{32}Fe_{68}$. Between 120 and 400 K, the specific heats of the two samples are nearly identical.

Figure 6 shows the specific heat of *sputtered* a-$Tb_{34}Fe_{66}$ grown at $T_s = 523$ K. Data are shown for the film as deposited and after annealing (520 K for approximately 2 h). The T_c is slightly lower (by 20 K) than that found for the evaporated samples, partially due to the increased Tb concentration, but the peak width is comparable. Annealing increases T_c slightly (by ~10 K) and causes the peak to sharpen, to even a greater degree than for the evaporated samples (compare, for example, the two samples grown at 523 K, Figs. 6

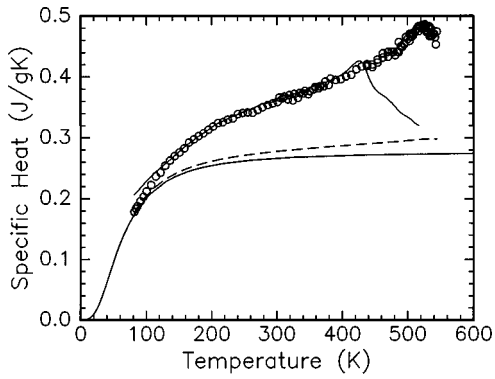

FIG. 5. Specific heat C_p for *e*-beam-evaporated *a*-$GdFe_2$ grown at $T_s = 348$ K as deposited. (Note that sample has effectively been annealed at 523 K by the measuring process.) Upper solid line shows C_p for *a*-$Tb_{32}Fe_{68}$ (from Fig. 2). Dashed line: estimated lattice ($\Theta_D = 260$ K), electronic ($\gamma = 7$ mJ/mol K), and dilation (see Ref. 62) contributions. Lower solid line: Debye harmonic contribution for $\Theta_D = 260$ K.

and 2 insets). We have also measured a sputtered film grown at 273 K as deposited and annealed and results are very similar:[51] the lower T_s results in a slightly lower T_c and a broader peak, which both sharpens and shifts to higher T_c (by ~10 K) upon annealing. Figure 7 shows a comparison of the specific heat of the sputtered films and one of the evaporated films.

For each of the data, the magnetic contribution to the specific heat $C_m(T)$ is determined by subtracting the lattice, electronic, and dilation contributions. The lattice contribution is constrained by the lower-temperature data in Figs. 1–7 to have a Debye temperature $\Theta_D > 230$ K for *a*-$Tb_{32}Fe_{68}$ and >260 K for *a*-$Gd_{32}Fe_{68}$.[60] An upper limit of $\Theta_D = 300$ K is set by thermodynamic measurements of crystalline $TbFe_2$ and $GdFe_2$.[61] $\Theta_D > 260$ K gave an unphysical temperature dependence to $C_m(T)$ for *a*-$Tb_{32}Fe_{68}$ (it increased with decreasing temperature below 100 K). It is likely that *a*-$TbFe_2$ and *a*-$GdFe_2$ have similar lattice contributions; we therefore used a Debye temperature $\Theta_D = 260$ K for both. For the electronic contribution, we use γT with $\gamma = 7$ mJ/mol K, the value determined from low-temperature specific heat measurements for *a*-YNi_2;[24] this contribution is approximately 2% of C_p at 500 K. The dilation contribution $C_p - C_v$ (also approximately 2% of C_p at 500 K) is estimated by using the semiempirical Nernst-Lindemann equation $C_p - C_v = AC_p^2T$, with $A = 3.3 \times 10^{-7}$ mol/J.[62] This construction yields the short-dashed lines shown in Figs. 2 and 5. $C_m(T)$ is the difference between the data and these lines. A minimum value for $C_m(T)$ is found for *a*-$Tb_{32}Fe_{68}$ by choosing the lowest possible Debye temperature (230 K) consistent with our lower-temperature measurements[60] (this maximizes the lattice contribution) and a maximum dilation and electronic contribution such that the total nonmagnetic contribution matches the lowest measured value of the specific heat at 525 K. The long-dashed line in Fig. 2 shows this calculation. An (unrealistic) upper limit for $C_m(T)$ for *a*-$Tb_{32}Fe_{68}$ is based on a minimum lattice contribution [$\Theta_D = 300$ K (Ref. 60)] and electronic γT only, with no dilation contribution. This line is not shown in the figure, but allows us to set an upper limit on magnetic entropy (discussed below).

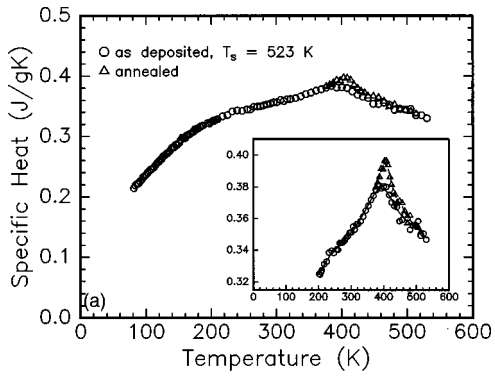

FIG. 6. Specific heat for sputtered *a*-$Tb_{34}Fe_{66}$ grown at $T_s = 523$ K [as deposited (○) and annealed between 450 and 540 K for approximately 2 h (△)]. $M = 440$ emu/cm^3, $K_u = 2.8 \times 10^6$ ergs/cm^3 as deposited, $= 1.9$ ergs/cm^3 annealed.

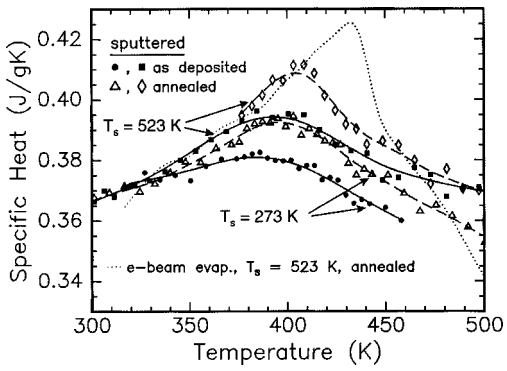

FIG. 7. Comparison of specific heat for sputtered *a*-$Tb_{34}Fe_{66}$ grown at $T_s = 523$ K (■ and ◊) and 273 K (● and △). Solid symbols are as deposited; open symbols are annealed. Dotted line shows comparison with *e*-beam-evaporated *a*-$Tb_{32}Fe_{68}$ grown at 523 K and annealed at 623 K for 4.5 h.

Figure 8 shows normalized $M(T)$ near T_c for the samples whose heat capacity data are shown in this paper. $M(T)$ was measured on heating in a 200 Oe field after first magnetizing the samples in a high field (10 kOe). The ''kink'' method for

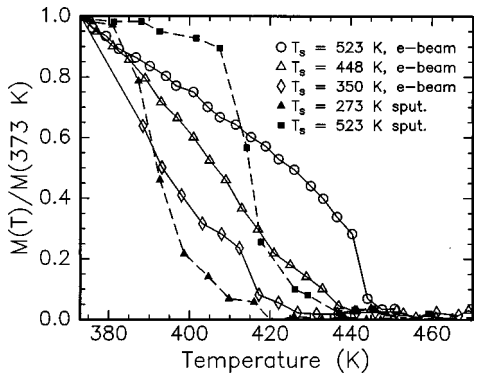

FIG. 8. $M(T)$ near T_c for *e*-beam-evaporated *a*-$Tb_{32}Fe_{68}$ grown at $T_s = 348$, 423, and 523 K and sputtered *a*-$Tb_{34}Fe_{66}$ grown at $T_s = 273$ and 523 K. All data normalized to value measured at 373 K. Data were taken on heating in a 200 Oe applied field normal to the sample plane after magnetically saturating the sample at room temperature with 10 kOe applied normal to the plane. Samples shown are from the same deposition runs as samples shown in Figs. 1–7.

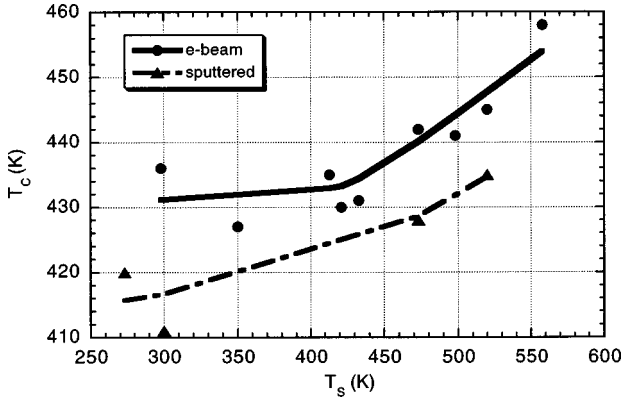

FIG. 9. T_c determined by kink method from plots such as those shown in Fig. 8 vs substrate temperature T_s for *e*-beam-evaporated *a*-$Tb_{32}Fe_{68}$ and sputtered *a*-$Tb_{34}Fe_{66}$. Samples grown at temperatures $T_s < 400$ K show signs of annealing (relaxation) upon measuring up to 480 K (necessary for measuring T_c); specifically, T_c increases by 10–15 K with a second measurement. T_c for these samples thus may be slightly shifted upwards from their intrinsic as-grown value.

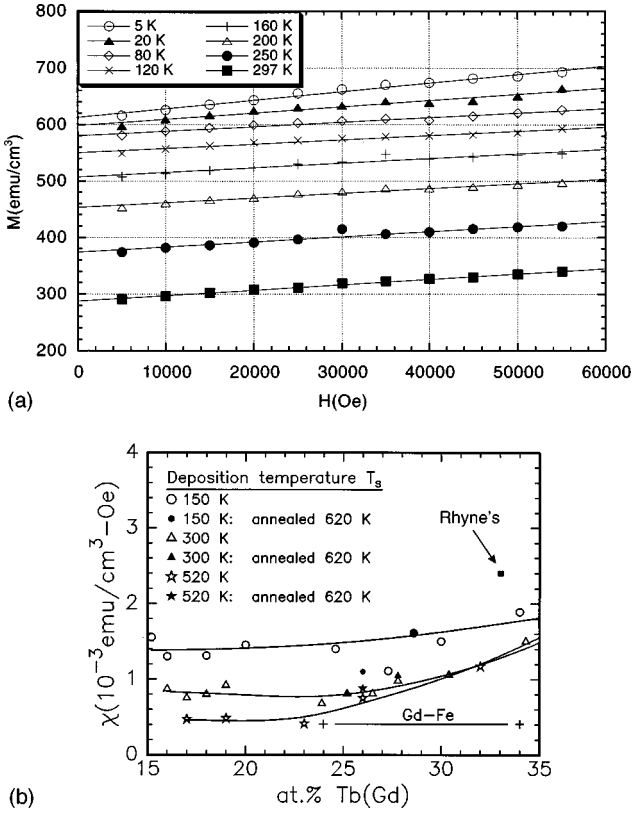

FIG. 10. (a) Magnetization of sputtered *a*-$Tb_{28}Fe_{72}$ grown at $T_s = 300$ K vs applied field at various measuring temperatures. Field applied normal to plane of film. All data taken on cooling in the applied field from room temperature. Coercive field H_c is 700 Oe at room temperature, and the sample is Tb rich of the room-temperature compensation composition; so all data are taken in the technically saturated state. Diamagnetic contribution of substrate and sample holder has been subtracted. Lines show fit to linear differential susceptibility ($M_0 + \chi H$). (b) High-field susceptibility $\chi = \partial M/\partial H$ at 300 K in fields to 5.5 T for sputtered *a*-Tb_xFe_{100-x} and *a*-Gd_xFe_{100-x} vs composition x for various T_s and anneals as shown (all anneals for 4 h). Data from Rhyne *et al.* (Ref. 9) for extremely rapidly sputtered *a*-$TbFe_2$ also shown. T_c varies very little over composition range shown in figure.

defining T_c from these data was used. T_c from this measurement correlates with the peak of the specific heat measurements, but is systematically ~10–15 K higher; this may reflect the breadth of the transition due to inhomogeneity in either density or atomic coordination or could be a thermometry calibration error in the magnetometer which relies on a thermocouple. Figure 9 shows this magnetically measured T_c versus growth temperature T_s for *a*-$Tb_{32}Fe_{68}$ samples grown by *e*-beam coevaporation and by sputtering. There is a systematic trend to higher T_c with increasing T_s, as seen in the specific heat measurements. A similar trend is found with annealing. There is no sign of crystallinity in these samples; the shifts in T_c are likely due to small changes in density and atomic coordination. We note that T_c for the crystalline Tb-Fe compounds with comparable composition are all much higher: 711 K for $TbFe_2$, 650 K for $TbFe_3$, and 574 K for Tb_6Fe_{23}.[37]

Figure 10(a) shows M vs H at various temperatures T from 297 K down to 5 K for sputtered *a*-$Tb_{28}Fe_{72}$. For this sample, $H_c = 700$ Oe at 297 K, and increases with decreasing T. The $M(H)$ loops are square, and the remanent moment in zero field equals the intercept from the high-field slope for all temperatures shown; i.e., the sample does not spontaneously demagnetize in zero field. The data in Fig. 10(a) are for field cooling, which puts the sample into the technically saturated state (no magnetic domains). Substrate and background (sample holder) susceptibility have been subtracted. The data show a significant positive (paramagnetic) high-field susceptibility $\chi = \partial M/\partial H$ above technical saturation. This differential susceptibility χ depends only weakly on H up to 5.5. Fitting with RMA-theory functional approaches to saturation [i.e., $(M_0 - M)/M_0 = \chi H + AH^{-0.5}$ or $\chi H + AH^{-2}$] (Ref. 20) did not appreciably improve the quality of the fits. χ does *not* depend strongly on T, although M_s, K_u, and H_c all have strong dependences on T. For the sample shown in Fig. 10(a), M_s varies by over a factor of 2 between 300 and 20 K, while χ varies by less than 20%. This lack of dependence of χ on T is consistent with earlier data of Rhyne for *a*-$Ho_{33}Fe_{67}$ and *a*-$Tb_{33}Fe_{67}$.[8]

Figure 10(b) shows the differential linear susceptibility χ versus composition x for sputtered *a*-Tb_xFe_{100-x} and *a*-Gd_xFe_{100-x} grown at different temperatures T_s. χ in this figure was measured at room temperature in fields to 5.5 T. There is a significant decrease in χ with increasing growth temperature; samples grown at the highest temperature (523 K) have χ nearly identical to the *a*-Gd_xFe_{100-x} sample. All values are lower (factor of 2) than that measured in the rapidly sputtered samples of Rhyne *et al.*, also shown in the figure.[8] χ for *a*-Tb_xFe_{100-x} slightly increases with increasing x at the higher values of x, but is nearly constant through the ferrimagnetic compensation point [$M(297\text{ K}) = 0$ for ~21 at. % Tb). χ is thus independent of the net magnetization and must therefore reflect a susceptibility of the sublattice moments, as originally suggested by Rhyne *et al.*[9] Annealing

did not result in any noticeable change in the magnitude of χ despite significant changes in K_u and H_c.

IV. DISCUSSION

The peak in the specific heat $C_p(T)$ is relatively sharp and occurs at a temperature T_c which is (if anything) slightly *lower* than that measured from the magnetization onset. These results are unlike conventional spin glasses where the specific heat maximum is at a temperature considerably higher than T_c determined from magnetization measurements and is quite broad, reflecting the development of short-range order only. Even for *S*-state Gd where we expect negligible RMA effects ($D/J_{ex} \ll 1$), we observe a $C_p(T)$ peak comparably sharp to the Tb-based alloy. Annealing or raising the growth temperature T_s increases T_c by 5–25 K depending on the original T_c and sharpens the $C_p(T)$ peak. It thus appears that the T_c of fully relaxed a-$TbFe_2$ is closer to 450 K than the 400 K usually quoted. The shift in T_c due to annealing or higher T_s for both sputtered and *e*-beam-evaporated samples is likely due to a small increase in density or changes in coordination, causing an increased exchange interaction. a-Tb_xFe_{1-x} samples prepared by *e*-beam evaporation show a slightly higher T_c (20 K approximately) than those prepared by sputtering at a comparable T_s. The reduced T_c of sputtered samples suggests that they are locally less dense (thereby lowering the exchange interaction) than the *e*-beam-evaporated samples. The sputtered samples also have a slightly lower K_u for each growth temperature T_s, evidence of less surface mobility during growth,[2,50] and the $C_p(T)$ peak sharpens more rapidly on annealing, evidence that in the bulk of the sample diffusion and relaxation occurs more readily, all consistent with a somewhat lower local density in the sputtered samples.

To further characterize the shape of the $C_p(T)$ peak, and hence the nature of the phase transition, we turn to critical exponent analysis and write $C_m = (A/\alpha)t^{-\alpha} + B$, a form appropriate for a negative value of α.[63] Figures 11 and 12 show log-log plots of $[C_m(T_c) - C_m(T)]$ versus reduced temperature $t = (T - T_c)/T_c$ above T_c and $t = (T_c - T)/T_c$ below T_c for a-$Tb_{32}Fe_{68}$. The fits made are not sensitive to the subtractions made to get C_m from C_p. T_c and $C_m(T_c)$ are fitting parameters; here they were chosen by eye from the raw data.[64] Data on samples prepared at other temperatures or for other annealing conditions are qualitatively similar. For all samples, α was found to be equal to α' and is approximately -0.6 to -0.7 and the critical amplitude ratio A/A' is approximately 2 (ranging from 1.5 to 2.7) (primed values: $T < T_c$; unprimed: $T > T_c$). For a-$GdFe_2$, we were unable to measure substantially above T_c, but below T_c we again find $\alpha' = -0.6$ with no sign of deviation from a straight line on this plot, although data become noisy for reduced temperatures less than 0.03. For the a-$Tb_{32}Fe_{68}$, we find no significant change in either A/A' or α upon annealing (which we note eliminates K_u), but the data on annealed samples follow the critical behavior to smaller reduced temperature t, i.e., closer to T_c, giving the appearance discussed earlier of a sharper $C_p(T)$ peak. Deviations from scaling occur for $t < 2 \times 10^{-2}$, which is within approximately 8 K of T_c.[65] Measurements of amorphous, soft magnetic materials found that $t > 0.1$ did not reflect critical behavior; it was suggested

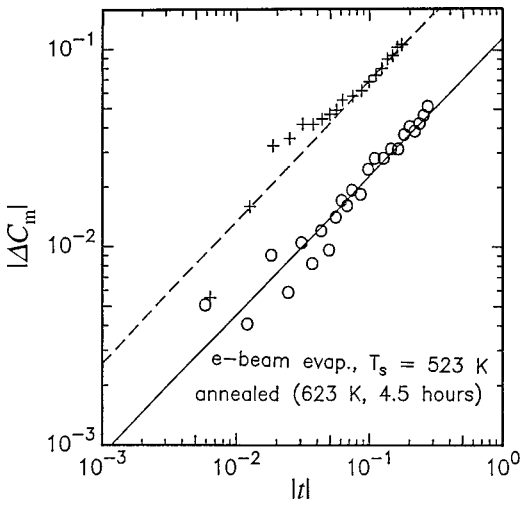

FIG. 11. Critical fluctuations plot for *e*-beam-evaporated sample grown at $T_s = 523$ K, shown in Fig. 2, annealed at 623 K for 4.5 h. Axes are $\log_{10}(\Delta C_m) = \log_{10}[C(T_c) - C(T)]$ and $\log_{10}(t) = \log_{10}[(T_c - T)/T_c]$ for $T < T_c$ (○) and $= \log_{10}[(T - T_c)/T_c]$ for $T > T_c$ (+). Slope $= -\alpha$. Intercept $= \log_{10}(-A/\alpha)$. $\alpha = \alpha' = -0.7$; $A/A' = 2.7$. (Primed values indicate $T < T_c$, unprimed values $T > T_c$.) Values before annealing were $\alpha = \alpha' = -0.6$, and amplitude ratio $A/A' = 2.7$.

that similar effects might be true for RMA magnets.[66] We however see no significant deviation in behavior for t on either side of this value. We suggest that samples, particularly those grown at lower growth temperatures, show a ''smearing'' of the C_p peak due to inhomogeneity such as density fluctuations. Annealing (without allowing crystallization) increases the homogeneity of the samples, causing them to show critical fluctuation behavior to smaller values of reduced temperature.

The apparent cusp in $C_p(T)$ and the near coincidence of the magnetically and thermodynamically determined T_c values suggest that we are observing a phase transition, for all samples, independent of the magnitude of K_u. The long-range order theoretically induced by K_u should cause the spins to be Ising like, instead of Heisenberg like, thus caus-

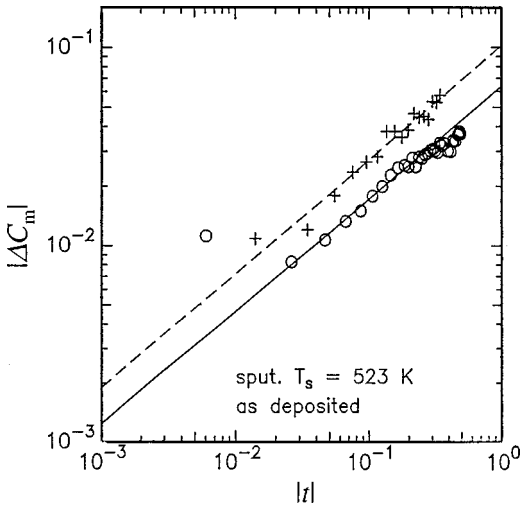

FIG. 12. Critical fluctuations plot for sputtered sample grown at $T_s = 523$ K, shown in Fig. 6, as deposited. Axes and symbols same as in Fig. 11. $\alpha = \alpha' = -0.6$. Amplitude ratio $A/A' = 1.5$. Values after annealing were $\alpha = \alpha' = -0.65$; $A/A' = 1.5$.

ing a phase transition to occur. However, we see similar behavior even in samples which have been annealed so that $K_u \sim 0$, or even further, so that the intrinsic anisotropy $K_{ui} = 0$ and resultant net anisotropy $K_u < 0$ due to shape anisotropy plus tensile strain-induced anisotropy which should give x-y ($m=2$) behavior. Our measured values of $\alpha \sim -0.6$ to -0.7 and $A/A' \sim 2$ are found in all samples. These observed exponents are significantly more negative than either Heisenberg or Ising phase transition exponents, but are also significantly less negative than that seen in spin glasses.[53] It is of course possible that inhomogeneity broadening obscures the real critical behavior at smaller t, such that the observed exponents are only effective critical exponents, representative of crossover behavior. von Molnar *et al.* and Hattori *et al.* also found a relatively sharp $C_p(T)$ peak at a temperature similar to that measured magnetically for a-Dy-Ni alloys and a-Er-Ni alloys, large-D/J_{ex} materials.[25,24] The value of α there appears to be between -2 and -1, significantly more negative than our present results on low-D/J_{ex} materials. These results together suggest that for RMA magnets with no significant exchange frustration, there is some form of phase transition at finite temperature, which is a qualitatively different behavior than that of a spin glass, consistent with observations based on magnetization.[39–42] By contrast, RMA magnets with randomness in the exchange as well as in the local anisotropy, such as a-Dy-Au and a-Dy-Cu alloys, show a broad $C_p(T)$ peak similar to the conventional spin glasses where exchange frustration dominates, and α, if it exists at all, is less than -2.[23–25]

As discussed in the Introduction, Fisch recently did a computer simulation on a two-component RMA system to approximate a low-D/J_{ex} material such as a-$TbFe_2$ and found a specific heat peak with an apparent cusp with $\alpha = -0.6$ and $A/A' = 2.5$, which is rounded (α more negative) for reduced temperatures below 0.05 (a value which depends strongly on D/J_{ex}), results strikingly similar to what we see experimentally.[31] The interpretation of these simulations is still somewhat unclear; changing x leads to changes in α and A/A',[31] inconsistent with universality theory. Fisch has suggested that the observed behavior is a crossover (as a function of concentration x) from pure Heisenberg model specific heat to random anisotropy behavior and that true critical behavior may only be visible for extremely small reduced temperatures. Further exploration of the dependence of the specific heat on concentration seems warranted.

The magnetic entropy S_{mag} developed between 80 and 525 K is determined from the specific heat by integrating C_m/T. We find $S_{mag} = 28 \pm 5$ J/mol K for a-$Tb_{32}Fe_{68}$ and 33 ± 5 J/mol K for a-$Gd_{32}Fe_{68}$; these numbers represent nearly all possible magnetic entropy for these materials. For spin glasses, typically less than 30% of the available magnetic entropy is developed between 0 K and magnetic freezing, and so this is further evidence that RMA materials do not behave like spin glasses. The uncertainty comes from the estimated uncertainties in electronic, lattice, and dilation contributions combined, plus a 5% uncertainty in sample mass. For a-$Tb_{32}Fe_{68}$, a firm lower limit on S_{mag} can be found by integrating the minimum $C_m(T)$ as discussed above and shown in Fig. 2: S_{mag} (lower limit) developed between 80 and 525 K $\sim$ 21 J/mol K. A firm upper limit is based on the upper limit on C_m discussed above; S_{mag} (upper limit) $= 32$ J/mol K. The magnetic entropy includes contributions from both Tb (or Gd) and Fe. Due to the low symmetry of the electrostatic field in an amorphous system, all orbital degeneracy is lifted with energy differences in the $3d$ transition series on the order of 10^4 K. The moment of the Fe is nonintegral in these metallic systems: $\mu \sim 1.6\mu_B$. Since this is nearly entirely a spin moment, with a g factor of 2, an approximation that is commonly used is to represent the available states as $2S+1 = 2.6$. Therefore, the contribution to the entropy by Fe_2 is $S_{mag} = 2R \ln 2.6 = 15.9$ J/mol K. For the $4f$ series, spin-orbit coupling is of the order of 10^4 K and the electrostatic field interaction is of the order of 10^2 K. L and S combine to give J, which is approximately still a good quantum number, and the crystal field (electrostatic) splittings will be given by $D[\langle J_z^2 \rangle - J(J+1)/3]$ with the z axis defined along the local $\hat{n}_i$ axis. For Tb ($J=6$), the entropy if all levels in the J multiplet were accessible would be $S_{mag} = R \ln 13 = 21.3$ J/mol K. Even for $D = 10$ K, almost certainly larger than the real value,[29] by 300 K the entropy S_{mag} for the Tb ion would be $R \ln 11.8$ if the energy levels were split by crystal fields only. By 525 K, $S_{mag} = R \ln 12.6$. These numbers imply that for a-$TbFe_2$ virtually all Tb crystal field levels should be occupied by 525 K and are significantly populated even by 300 K, quite unlike the early work done on a-DyCu where an observed entropy of only $R \ln 2$ through T_c led to the conclusion that only the lowest crystal field levels are populated. The random orientations of the crystal fields and the HPZ approximation of local uniaxial symmetry should not qualitatively change the argument that, by 525 K, crystal field splittings of a-$TbFe_2$ are not relevant and hence we expect to see the full magnetic entropy of the J multiplet. In a-$TbFe_2$, the exchange splitting of a single Tb ion at $T=0$ is larger than the crystal field splitting (another way of discussing $D/J_{ex} < 1$); hence the development of entropy is dominated by the usual excitations of a ferromagnetic system, e.g., spin waves. 525 K is far enough above $T_c = 420$ K that nearly all magnetic entropy should be developed. Thus the total expected entropy from $T=0$ to 525 K should be only slightly less than $(2R \ln 2.6 + R \ln 13) = 37$ J/mol K. The measured value between 80 and 525 K is 28 J/mol K; we therefore estimate that nearly 9 J/mol K is found below 80 K. For a-$GdFe_2$, the total theoretical magnetic entropy is $2R \ln 2.6 + R \ln 8 = 33$ J/mol K; the measured value is 33 ± 4 J/mol K between 80 and 525 K. Very little entropy must lie below 80 K therefore. We suggest that the low-temperature excitations for both of these materials, with D/J_{ex} ratios <1, will be dominated by spin-wave-like contributions. The smaller low-temperature (<80 K) magnetic contribution for a-$GdFe_2$ is consistent with the factor of 2 increase in J_{ex} (Gd-Fe) compared to (Tb-Fe).[4,67,68]

Finally, Figs. 10(a) and 10(b) show that the high-field magnetic susceptibility χ shows a strong correlation with growth temperature and a weak dependence on measurement temperature. We suggest that the dependence of χ on growth temperature is because the orientational correlation length R_a is longer in samples grown at higher temperature. This correlation can be extended to the early data of Rhyne *et al.*, for which $\chi = 2.2 \times 10^{-3}$ emu/cm^3 Oe.[9] We suggest that the extremely rapid sputtering rates ($\sim$100 Å/s) used to prepare

these earlier mm-thick a-$TbFe_2$ samples led to a less ordered amorphous sample, with slightly reduced T_c (383 K), no perpendicular anisotropy K_u, and a shorter R_a. The sample shown in Fig. 10(a) has perpendicular anisotropy K_u and has been magnetized with net out-of-plane remanent magnetization at zero field; it must therefore be in the ferromagnet with wandering axis (FWA) state at all fields shown. In this state, the angular deviation of the net magnetic moment from perpendicular varies inversely with the orientational correlation length R_a and χ varies in proportion with this angle. The observation that the high-field susceptibility χ does not change appreciably upon annealing, despite large changes in uniaxial anisotropy constant K_u, implies that structural relaxation of the amorphous state does not significantly affect R_a (and therefore R_f). There is an alternate interpretation for this high-field susceptibility: a ferrimagnetic-like canting of both Tb *and* Fe moments towards the field direction, due to weaker Tb-Fe exchange coupling. Given a long R_f, it is possible that both Tb and Fe moment directions wander. Following the geometry of Ref. 69 and assuming a wandering axis angle of as little as 10° from perpendicular, due to either macroscopic growth-induced effects or the random anisotropy-induced wandering, and using the mean-field values of the exchange constants, we obtained $\chi = 1 \times 10^{-3}$ ergs/cm^3 Oe for $H = 100$ kOe, a value consistent with observation. Finally, we have not subtracted a conduction electron susceptibility from χ, but it is very unlikely that this significantly depends on the preparation temperature. It is possible that the low values for a-$GdFe_2$ and a-$Tb_{32}Fe_{68}$ prepared at the highest temperatures reflect this contribution, and this should then be subtracted from the other data to give the true local moment contribution.

V. SUMMARY

We have shown that the magnetic ordering of a-RFe_2 thin films, where $R = $ Gd, Tb, shows a relatively sharp cusp in the specific heat, with evidence of thermodynamic critical fluctuations, at the same temperature as that measured magnetically, independent of the magnitude of coherent anisotropy K_u. a-$TbFe_2$ is considered a random-anisotropy magnet, in the exchange-dominated low-D/J_{ex} regime, while a-$GdFe_2$ has negligible anisotropy. Nonetheless, the specific heat of these two alloys appear nearly identical over most of the temperature range measured. Virtually all available magnetic entropy is evolved below T_c for both materials, quite unlike what is seen in spin glasses and unlike what was found for the high-D/J_{ex} materials where the low T_c led to the population of only the lowest crystal field levels. Fits to critical fluctuation theory suggest that the specific heat critical exponent α is approximately -0.6, significantly less negative than that found for high-D/J_{ex} materials, which are in turn significantly less negative than the upper limit set for spin glasses. From recent work by Fisch, it appears that $\alpha = -0.6$ may represent crossover behavior rather than a true critical exponent, with critical behavior only visible extremely close to T_c for low-D/J_{ex} materials. Sputtered and e-beam-evaporated a-RFe_2 samples appear qualitatively similar; there are small shifts in T_c which suggest that the evaporated films are locally denser, despite TEM evidence of larger scale density variations in the evaporated samples. Increasing the growth temperature of either sputtered or e-beam-evaporated samples causes a slight increase in T_c, a sharpening of the specific heat peak, and a decrease in high-field susceptibility χ. We suggest that this correlation can be understood by assuming that increasing the growth temperature increases the local density and the orientational correlation length R_a and improves the sample homogeneity which causes critical behavior to persist closer to T_c. Annealing of any sample also increases T_c and causes the specific heat peak to sharpen, due again to a more homogeneous, denser sample; χ, however, is unaffected, suggesting that R_a is not significantly changed.

ACKNOWLEDGMENTS

We would like to thank R. Fisch, E. M. Chudnovsky, J. M. D. Coey, R. Robinson, and J. J. Rhyne for valuable discussions, Darrell Denlinger and Kim Allen for fabricating the microcalorimeters, and Ken Takano, Karen Kavanaugh, Robert Opila, Julia Phillips, Chris Roudin, Richard Kodama, and Ricky Chau for their invaluable help in characterizing these samples. A special thanks goes to E. M. Gyorgy for his encouragement and insight in all areas of magnetism. We thank the DOE (DE-FG03-95ER45529) for support and gratefully acknowledge use of magnetometers at CMRR and CIMS at UCSD.

*Present address: Toyota Technological Institute, Nagoya, Japan.

[1] N. Heiman, A. Onton, D. F. Kyser, K. Lee, and C. R. Guarnieri, in *Magnetism and Magnetic Materials*, edited by C. D. Graham, G. H. Lander, and J. J. Rhyne, AIP Conf. Proc. No. **24** (AIP, New York, 1975), p. 573; R. J. Gambino, J. Ziegler, and J. J. Cuomo, Appl. Phys. Lett. **24**, 99 (1974).

[2] F. Hellman and E. M. Gyorgy, Phys. Rev. Lett. **68**, 1391 (1992); F. Hellman, R. B. van Dover, S. Nakahara, and E. M. Gyorgy, Phys. Rev. B **39**, 10 591 (1989), and references therein.

[3] R. B. van Dover, M. Hong, E. M. Gyorgy, J. F. Dillon, Jr., and S. D. Albiston, J. Appl. Phys. **57**, 3897 (1985).

[4] P. Hansen, C. Clausen, G. Much, M. Rosenkranz, and K. Witter, J. Appl. Phys. **66**, 756 (1989); D. Mergel, H. Heitmann, and P. Hansen, Phys. Rev. B **47**, 882 (1993).

[5] V. G. Harris, K. D. Aylesworth, B. N. Das, W. T. Elam, and N. C. Koon, Phys. Rev. Lett. **69**, 1939 (1992); IEEE Trans. Magn. **MAG-20**, 2958 (1992).

[6] S. N. Cheng and M. H. Kryder, J. Appl. Phys. **69**, 7202 (1991) and references therein.

[7] P. Hansen and H. Heitmann, IEEE Trans. Magn. **MAG-25**, 4390 (1989).

[8] J. J. Rhyne, S. J. Pickart, and H. A. Alperin, Phys. Rev. Lett. **29**, 1562 (1972); S. J. Pickart, J. J. Rhyne, and H. A. Alperin, *ibid.* **33**, 424 (1974); J. J. Rhyne, IEEE Trans. Magn. **MAG-21**, 1990 (1985).

[9] J. J. Rhyne, J. H. Schelleng, and N. C. Koon, Phys. Rev. B **10**, 4672 (1974).

[10] D. P. Belanger and A. P. Young, J. Magn. Magn. Mater. **100**, 272 (1991); K. Binder and A. P. Young, Rev. Mod. Phys. **58**, 801 (1986).

[11] K. Moorjani and J. M. D. Coey, *Magnetic Glasses* (Elsevier, New York, 1984).
[12] R. Harris, M. Plischke, and M. J. Zuckermann, Phys. Rev. Lett. **31**, 160 (1973).
[13] Yadin Y. Goldschmidt, in *Recent Progress in Random Magnets*, edited by D. H. Ryan (World Scientific, Singapore, 1992), p. 151.
[14] D. J. Sellmyer and M. J. O'Shea, in *Recent Progress in Random Magnets*, edited by D. H. Ryan (World Scientific, Singapore, 1992), p. 71.
[15] Eugene M. Chudnovsky, in *The Magnetism of Amorphous Metals and Alloys*, edited by J. A. Fernandez-Baca and Wai-Yim Ching (World Scientific, 1995), Chap. 3, p. 143.
[16] Y. Imry and S.-K. Ma, Phys. Rev. Lett. **35**, 1399 (1975).
[17] R. A. Pelcovits, E. Pytte, and J. Rudnick, Phys. Rev. Lett. **40**, 476 (1978); R. A. Pelcovits, Phys. Rev. B **19**, 465 (1979).
[18] C. Jayaprakash and S. Kirkpatrick, Phys. Rev. B **21**, 4072 (1980).
[19] Y. Goldschmidt and A. Aharony, Phys. Rev. B **32**, 264 (1985).
[20] E. M. Chudnovsky and R. A. Serota, IEEE Trans. Magn. **MAG-20**, 1400 (1984); J. Phys. C **16**, 4181 (1983); E. M. Chudnovsky, W. M. Saslow, and R. A. Serota, Phys. Rev. B **33**, 251 (1986).
[21] J. M. D. Coey and S. von Molnar, J. Phys. (France) Lett. **39**, L-327 (1978).
[22] J. M. D. Coey, T. R. McGuire, and B. Tissier, Phys. Rev. B **24**, 1261 (1981).
[23] J. M. D. Coey, S. von Molnar, and R. J. Gambino, Solid State Commun. **24**, 167 (1977).
[24] Y. Hattori, K. Fukamichi, K. Suzuki, H. Aruga-Katori, and T. Goto, J. Phys.: Condens. Matter **7**, 4193 (1995).
[25] S. von Molnar, T. R. McGuire, R. J. Gambino, and B. Barbara, J. Appl. Phys. **53**, 7666 (1982).
[26] D. W. Denlinger, E. N. Abarra, K. Allen, P. W. Rooney, M. T. Messer, S. K. Watson, and F. Hellman, Rev. Sci. Instrum. **65**, 946 (1994).
[27] J. P. Rebouillat, A. Lienard, J. M. D. Coey, R. Arrese-Boggiano, and J. Chappert, Physica B **86–88**, 773 (1977); J. W. M. Biesterbos, M. Brouha, and A. G. Dirks, *ibid.* **86–88**, 770 (1977).
[28] R. Fisch, Phys. Rev. B **41**, 11 705 (1990); **42**, 540 (1990).
[29] The ratio D/J_{ex} (or A/K_r) is complicated in a material with two magnetic ions, one (Tb) with strong anisotropy and the other (Fe) giving the strong exchange which produces a T_c well above room temperature. From mean-field analyses (Refs. 4, 67, and 68), Fe-Fe exchange is the largest, Tb-Fe exchange is approximately 1/3 of this, and Tb-Tb exchange is extremely small. The most appropriate J_{ex} is the Fe-Tb coupling constant, $\sim 1.0-1.5\times10^{-15}$ ergs. Then the effective value for A is $\sim 0.7-1.0\times10^{-6}$ ergs/cm. [$A=4J_{ex}JS/\sqrt{2}d$, where $J=6$ for Tb, $S=1$ for Fe, and d refers to the Tb-Fe distance $\sim 2.5\times10^{-8}$ cm. The factors of 4 and $\sqrt{2}$ are numerical factors chosen by comparison to an fcc close-packed structure ($4/a$ is the usual formula where $a=$ fcc lattice constant).] Values for D for Dy (Tb should be comparable) in a-Dy-Ni alloys range from 3 to 5 K $=4-7\times10^{-16}$ ergs. For $D=4-7\times10^{-16}$ ergs, $K_r=DN_{Tb}J^2=2.6-4.5\times10^8$ ergs/cm^3 at $T=0$ K ($N_{Tb}=1.8\times10^{22}$ cm^{-3}, based on 8.3 g/cm^3 and 33 at. % Tb concentration). For a-$TbFe_2$, the observed macroscopic anisotropy K_u is as large as 1×10^7 ergs/cm^3 at room temperature and approximately 3 times larger at low temperatures (see, e.g., Ref. 9). K_r is thus somewhat more than a factor of 10 larger than K_u, a reasonable upper limit given the amorphous structure, where the alignment of axes is unlikely to be larger than a few percent. For $D=4-7\times10^{-16}$ ergs and $J_{ex}=1-1.5\times10^{-15}$ ergs, $D/J_{ex}=0.3-0.7$ and $H_r/H_{ex}=(K_r/A)R_a^2\sim0.1-0.4$ for $R_a=2.5$ Å. If the orientational correlation length R_a is longer, the effective value of D/J_{ex} is increased by $(R_a/a)^2$, a factor which could be large. $R_f=50$ Å at low temperature from Ref. 8 gives $R_a\sim2.3$ Å $\sim$ interatomic spacing, assuming $A\sim0.7-1\times10^{-6}$ ergs/cm and $K_r=DN_{Tb}J^2\sim4\times10^8$ ergs/cm^3. The number of neighbors should also affect the relevant D/J_{ex} ratio; however, the number of Fe neighbors for Tb in a-$TbFe_2$ is similar to the number of magnetic neighbors in other RMA materials studied. A factor of 3 makes little difference to any of the discussion in this paper; due to the strong Tb-Fe exchange coupling, these alloys are in the moderately weak anisotropy limit unless R_a is much longer than the interatomic spacing.
[30] R. Fisch and A. B. Harris, Phys. Rev. B **41**, 11 305 (1990).
[31] R. Fisch, following paper, Phys. Rev. B **58**, 5684 (1998).
[32] B. Barbara and B. Dieny, Physica B **130**, 245 (1985).
[33] J. M. D. Coey, J. Appl. Phys. **49**, 1646 (1978).
[34] Ronald Fisch, Phys. Rev. B **51**, 11 507 (1995); Phys. Rev. Lett. **66**, 2041 (1991).
[35] R. Fisch, Phys. Rev. B **57**, 269 (1998).
[36] K. M. Lee and M. J. O'Shea, Phys. Rev. B **48**, 13 614 (1993).
[37] James J. Rhyne, in *Handbook on the Physics and Chemistry of Rare Earths*, edited by Karl A. Gschneidner, Jr. and L. Eyring (North-Holland, New York, 1979), Vol. 16, p. 259.
[38] J. Filippi, B. Dieny, and B. Barbara, Solid State Commun. **53**, 523 (1985).
[39] D. J. Sellmyer and S. Nafis, Phys. Rev. Lett. **57**, 1173 (1986); J. Appl. Phys. **57**, 3584 (1985).
[40] B. Dieny and B. Barbara, Phys. Rev. Lett. **57**, 1169 (1986).
[41] K. M. Lee and M. J. O'Shea, J. Appl. Phys. **67**, 5781 (1990).
[42] K. M. Lee, M. J. O'Shea, and D. J. Sellmyer, J. Appl. Phys. **61**, 3616 (1987).
[43] R. Reisser, M. Seeger, and H. Kronmüller, J. Magn. Magn. Mater. **128**, 321 (1993).
[44] D. R. Nelson, J. Non-Cryst. Solids **61–62**, 475 (1984).
[45] E. M. Chudnovsky and J. Tejada, Europhys. Lett. **23**, 517 (1993).
[46] J. M. Ruiz, X. X. Zhang, C. Ferrater, and J. Tejada, Phys. Rev. B **52**, 10 202 (1995).
[47] A. B. Harris, J. Phys. C **7**, 1671 (1974).
[48] A. del Moral, J. I. Arnaudas, P. M. Gehring, M. B. Salamon, C. Ritter, E. Joven, and J. Cullen, Phys. Rev. B **47**, 7892 (1993).
[49] T. Saito, H. Miyano, K. Shinagawa, and T. Tsushima, J. Magn. Magn. Mater. **140–144**, 1757 (1995).
[50] F. Hellman, Appl. Phys. Lett. **64**, 1947 (1994).
[51] For the *e*-beam-evaporated samples, see E. N. Abarra, Ph.D. thesis, University of California at San Diego, 1996.
[52] Working in Chudnovsky's notation, using the numbers from Ref. 29, $H_c/H_s=K_uA^3/K_r^4R_a^6=K_uR_f^2/A=1$ for $K_u=3.0-4.0\times10^6$ ergs/cm^3 at $T=0$ K, assuming $R_f=50$ Å from Rhyne's measurements. Using the measured value of R_f leads to less uncertainty than the separate values of A, K_r, and R_a.
[53] F. L. Lederman, M. B. Salamon, and L. W. Shacklette, Phys. Rev. B **9**, 2981 (1974).
[54] G. S. Cargill and S. Kirkpatrick, in *Structure and Excitations of Amorphous Solids*, edited by G. Lucovsky and F. L. Galeener, AIP Conf. Proc. No. **31** (AIP, New York, 1976), p. 339.
[55] For the sputtered samples, see Refs. 2 and 3; also F. Hellman, S. Nakahara, R. P. Frankenthal, R. B. van Dover, D. J. Siconolfi, and E. M. Gryogy, J. Appl. Phys. **65**, 2847 (1989).
[56] J-W. Lee, H-P. D. Shieh, M. H. Kryder, and D. E. Laughlin, J.

Appl. Phys. **63**, 3624 (1988); F. Hellman and K. Kavanagh (unpublished TEM work on amorphous Gd-Si); also see, for example, A. G. Dirks and H. J. Leamy, Thin Solid Films **47**, 219 (1977); N. G. Nakhodkin and A. I. Shaldervan, *ibid.* **10**, 109 (1972); J. A. Thornton, J. Vac. Sci. Technol. **12**, 830 (1975); and recent conferences on kinetic roughening.

[57] H. Miyajima, K. Sato, and T. Mizoguchi, J. Appl. Phys. **47**, 4669 (1976).

[58] The composition for the a-$GdFe_2$ sample was based on deposition rates and magnetization measurements only. No microprobe was done.

[59] M. Moske and K. Samwer, Z. Phys. B **77**, 3 (1989).

[60] $\Theta_D < 230$ K for a-$Tb_{32}Fe_{68}$ would imply a lattice contribution greater than the total heat capacity at 100 K, from measurements shown in Fig. 2. For a-$Gd_{32}Fe_{68}$ the lower limit is 260 K. $\Theta_D > 260$ K gives an unphysical temperature dependence to $C_m(T)$ for a-$Tb_{32}Fe_{68}$ (it increases with decreasing temperature below 100 K). See Ref. 33 for a similar analysis for a-Dy-Cu alloys where they found $\Theta_D = 190$ K. Hattori *et al.* (Ref. 24) determined $\Theta_D = 200$ K for a-$ErNi_2$.

[61] D. J. Germano, R. A. Butera, and K. A. Gschneidner, Jr., Solid State Chem. **37**, 383 (1981); R. A. Butera, T. J. Clinton, A. G. Moldovan, S. G. Sankar, and K. A. Gschneidner, Jr., J. Appl. Phys. **50**, 7492 (1979).

[62] The dilation contribution $C_p - C_v = V_m \beta^2 T / K_T \equiv A C_p^2 T$, where V_m is the molar volume, $\beta = 3\alpha =$ thermal expansion coefficient, K_T is the isothermal compressibility, and $A = V_m \beta^2 / C_p^2 K_T$ is a combination of these parameters [see, e.g., F. Reif, *Fundamentals of Statistical and Thermal Physics* (McGraw-Hill, New York, 1965), p. 168]. It has been empirically found that the value for A is approximately constant with T, so that a determination of all components at one temperature allows an estimate of dilation at all temperatures [W. Nernst and F. A. Lindemann, Z. Elektrochem. **17**, 817 (1911); A. P. Miller, *Cindas Data Series on Material Properties Specific Heat of Solids* (Hemisphere Publ. Corp., New York, 1988), Vols. 1 and 2]. We determined the constant A at 300 K, where C_p for a-$TbFe_2$ and a-$GdFe_2$ are nearly identical. A mole in this paper is defined as a mole of $TbFe_2$ ($GdFe_2$); thus $V_m = (271\ \text{g/mol})/(8.3\ \text{g/cm}^3) = 32.6\ \text{cm}^3/\text{mol}$ ($32.4\ \text{cm}^3/\text{mol}$). We used $K_T = 2.6 \times 10^{-12}$ cm^2/dyn for both (based on crystalline Gd, which has a similar Θ_D). For β, we used $\alpha = 1.67 \times 10^{-5}\ \text{K}^{-1}$ measured for crystalline $GdCo_2$ [from Y. S. Touloukian, R. K. Kirby, R. E. Taylor, and P. D. Desai, *Thermal Expansion Metallic Elements and Alloys, Thermophysical Properties of Matter* Vol. 12 (Plenum, New York, 1970), p. 509]. For a-$TbFe_2$ and a-$GdFe_2$ this gives a value of $A = 3.3 \times 10^{-7}$ mol/J.

[63] V. Privman, P. C. Hohenberg, and A. Aharony, in *Phase Transitions and Critical Phenomena*, edited by C. Domb and J. L. Lebowitz (Academic, London, 1991), Vol. 14, p. 1.

[64] If instead C_{total} is fit, $\alpha = \alpha' \approx -0.5$ for the $T_s = 523$ K evaporated sample. T_c and $C_m(T_c)$ were chosen such that $\alpha\ (T > T_c) = \alpha'\ (T < T_c)$ over the longest possible span in t. For example, for the unannealed evaporated sample ($T_s = 523$ K), $T_c = 428$ K, which is within 1 K of the peak determined by eye, and $C_m(T_c) = 0.121$, which is within 1% of the measured value at T_c. α is sensitive to the choice of T_c; for example, a 1% change in T_c (<5 K) results in a 10–13 % change in α and α'. α is not as sensitive to the value chosen for $C_m(T_c)$; a 1% change in $C_m(T_c)$ causes a 2–4 % change in α.

[65] Our experimental technique cannot resolve better than reduced temperatures of 3×10^{-3}, the magnitude of the temperature excursion used for the heat capacity measurement.

[66] M. Fahnle, W.-U. Kellner, and H. Kronmuller, Phys. Rev. B **35**, 3640 (1987).

[67] A. Gangulee and R. C. Taylor, J. Appl. Phys. **49**, 1762 (1978); A. Gangulee and R. J. Kobliska, *ibid.* **49**, 4896 (1978).

[68] M. Mansuripur and M. F. Ruane, IEEE Trans. Magn. **MAG-22**, 33 (1986).

[69] F. Hellman, Appl. Phys. Lett. **59**, 2757 (1991).